Combined effect of moisture and test temperature on the pseudo-ductility of thin-ply carbon/epoxy-glass/epoxy hybrid composites

Czél G. , Bugár-Mészáros M., Wisnom M. R.

Combined effect of moisture and test temperature on the pseudo-ductility of thin-ply carbon/epoxy-glass/epoxy hybrid composites

Gergely Czél [a],[*], Márton Bugár-Mészáros [a], Michael R. Wisnom [b]

[a] *Department of Polymer Engineering, Faculty of Mechanical Engineering, Budapest University of Technology and Economics, Műegyetem rkp, 3, Budapest 1111, Hungary*
[b] *Bristol Composites Institute, University of Bristol, Queen's Building, University Walk, Bristol BS8 1TR, United Kingdom*

ARTICLE INFO

ABSTRACT

Two different glass/carbon fibre-epoxy interlayer hybrid composite specimen types (with continuous or discontinuous carbon layer) were investigated. Unconditioned and conditioned composite specimens were tested at various temperatures in order to study the temperature dependency and moisture sensitivity of the tensile and interlaminar properties of the hybrid composites. The tensile response of the unconditioned continuous specimens was barely influenced by temperature and the specimens failed in pseudo-ductile mode. The unconditioned discontinuous specimens delaminated stably at the glass/carbon interface. Increasing the test temperature from $-50\ °C$ to $80\ °C$, the mode II fracture toughness of glass/carbon hybrid composites decreased significantly. The effect of moisture significantly changed the behaviour of both type hybrid composites at all temperatures leading to unstable delamination and glass fibre failure as well. The main reason for this was the decrease in strength of the S-glass/epoxy layers.

1. Introduction

High performance carbon fibre reinforced polymer composites are known to have excellent mechanical properties including high strength and stiffness, low density, corrosion resistance and therefore these materials are commonly used in applications such as defence and civil aviation, space and motorsports. Despite the attractive properties of composites, their application is limited in several safety–critical fields by sudden and catastrophic failure without sufficient warning and residual load bearing capacity.

There are numerous approaches to overcome the brittle, abrupt failure of high performance composites. One of the promising solutions is the application of novel, ductile fibre types e.g. carbon nanotube or nanofibrillated cellulose (NFC) fibres [1,2], however their development and commercialization is not only time consuming but also requires a great amount of effort and is still underway. Stainless steel fibre reinforced composites [3,4] are reported to have ductile, progressive failure in comparison with conventional unidirectional (UD) glass and carbon fibre reinforced composites, but their use may be limited in weight-critical applications due to the high density of steel fibres. Nevertheless, the hybridization of steel and carbon/glass fibres might be interesting in safety critical fields of industry where product mass plays a

secondary role.

Another approach to enhance ductility is to tailor the damage mechanism of the composite. A key factor in the damage mechanism design is the ply thickness of the material. Thin-ply angle-ply carbon /epoxy (CF/EP) composites [5,6] showed non-linear pseudo-ductile failure as a result of fibre rotation and non-linear shear deformation of the matrix. Thin-ply angle-ply composites are less sensitive to delamination, which is commonly responsible for the premature failure of standard thickness angle-ply composites, thereby metal-like yielding can be achieved with tensile failure strains beyond 10 %. Fibre hybridization at ply level [7–11] can also lead to pseudo-ductile failure. Thin-plies release less energy at ply fracture than standard thickness plies. Hence if the energy release rate at the first fracture in the thin, low elongation (LE) layer of an interlayer (or layer-by-layer, sandwich) hybrid composite is lower than the fracture toughness of the interface between the LE and high elongation (HE) material layers, then fragmentation of the LE layer and dispersed stable delamination between the HE and LE layer can take place. This progressive damage mechanism provides a clear warning before final failure which is indicated by a plateau in the stress–strain curve after the initial linearly increasing section. The lack of delamination allows the carbon layer to fragment multiple times, resulting in a progressive damage process that is visible due to the

translucent nature of the glass layers [7]. Non-linear tensile responses of UD thin-ply glass/carbon hybrids [8,9], high modulus (HM)/high strength (HS) carbon–carbon hybrids [10] and quasi-isotropic (QI) HM/HS carbon–carbon hybrids [11] have been demonstrated at room temperature by Czél et al. While the response was investigated under standard laboratory conditions, the tensile behaviour of thin-ply glass/carbon hybrids exposed to the combination of temperature and moisture has not previously been examined in detail.

The longitudinal tensile strength of high performance UD CF/EP composites is reported to be insensitive to the test temperature well below the glass transition temperature (T_g) of the matrix [12–18]. On the other hand, if the test temperature is elevated above T_g, the tensile strength of CF/EP composites greatly decreases due to the softening of the thermoset resin. Koma et. al [16] found that the lower the modulus of the carbon fibre the higher the strength degradation of carbon/epoxy composites at temperatures close to or over T_g. Wet or hot-wet conditioning reduces the T_g of the matrix and possibly initiates an earlier strength degradation compared to unconditioned specimens at test temperatures around T_g. Some of the authors reported that hot-wet conditioning did not or only slightly affected the longitudinal tensile strength of carbon fibre reinforced composites [18–20], whilst others found that hot-wet conditioning decreased the tensile strength remarkably [21–23]. This discrepancy is probably due to the wide range of materials examined under different conditions. Test temperatures below T_g have no significant effect on the tensile strength of glass fibre/epoxy (GF/EP) composites [24]. However, the tensile properties of GF/EP composites are greatly influenced by hot-wet conditioning; serious strength reductions (25–50 %) have been reported by numerous authors [25–28].

The effect of temperature and moisture on the interlaminar properties of fibre reinforced composites was extensively studied [20,29–35]. In general, both temperature elevation and moisture absorption typically decrease the mode II fracture toughness (G_{IIC}) of composite materials. Both environmental effects plasticize the matrix material that plays a key role in the failure mechanisms of composites under pure mode II loading.

The aim of this paper is to present the results of a detailed study on the effects of test temperature and exposure to high relative humidity on the mechanical properties of pseudo-ductile glass/carbon-epoxy hybrid composites. The two dominant damage modes i.e. CF/EP layer fragmentation and delamination are studied separately.

2. Experimental

2.1. Materials

For the experiments Tairyfil TC35 carbon fibres and Y-110 S-2 glass fibres were used as LE and HE fibres respectively. UD thin-ply CF/EP pre-impregnated composite sheets (prepregs) and standard thickness S-glass/epoxy (SGF/EP) prepregs were supplied by SK Chemicals and Hexcel, respectively. The epoxy resin matrices in the prepregs were the general purpose toughened K50 (SK Chemicals) and the aerospace grade 913 (Hexcel). The basic properties of the applied fibres and prepregs are collected in Tables 1 and 2.

2.2. Specimen design

In the present study-two different UD hybrid specimen configurations were used. The continuous specimens ([S-glass$_1$/TC35-carbon$_2$/S-glass$_1$]) consisted of two carbon plies in the central layer and one glass ply on each side of the carbon layer (Fig. 1/a). In the case of these continuous specimens, fragmentation of the carbon layer along the gauge length and localized delamination near the cracks were expected. In order to promote delamination, the discontinuous specimens ([S-glass$_2$/TC35-carbon(cut)$_4$/S-glass$_2$]) were made with double thickness for each layer and the central carbon plies were cut in the middle (Fig. 1/

Table 1
Fibre properties of the applied UD prepregs based on manufacturer's data.

Fibre type (Manufacturer)	Elastic modulus [GPa]	Strain to failure [%]	Tensile strength [GPa]	Coefficient of thermal expansion[a] [1/°C]	Density [g/cm³]
Tairyfil TC35 carbon (Formosa)	240	1.6	4.0	−4.1·10⁻⁷	1.80
Y-110 S-2 glass (AGY)	89	5.7	4.9	3.4·10⁻⁶	2.47

[a] Estimated values, based on general literature or data for similar fibre types

b). The cut was introduced in the uncured carbon/epoxy prepreg layer with a rotary blade by hand during the lay-up of the test plates. Those specimens containing discontinuous carbon layer were designed to develop delamination between the glass and carbon layers starting from the central cut, resulting in stable pull-out of the carbon layer [36].

The interface between the glass and carbon layer is under shear loading (pure mode II) when the central carbon layer is discontinuous. When the strain energy release rate exceeds the G_{IIC} of the material, delamination between the glass and carbon layers starts to propagate from the central cut. Basic calculations were carried out (according to [8]) to determine the expected initial elastic modulus of the hybrid specimens (E_h):

$$E_h = \frac{E_g \cdot 2 \cdot t_g + E_c \cdot t_c}{h} \tag{1}$$

where E_g is the longitudinal elastic modulus of the cured glass/epoxy composite, t_g is the nominal thickness of one glass layer, E_c is the longitudinal elastic modulus of the cured carbon/epoxy composite, t_c is the nominal thickness of the carbon layer and h is the overall thickness of the specimen. The mode II energy release rate (G_{II}) at a given strain in both type hybrid composite specimens (see Fig. 1) can be calculated using the following formula [8]:

$$G_{II} = \frac{\varepsilon_c^2 \cdot E_c \cdot t_c (E_g \cdot 2 \cdot t_g + E_c \cdot t_c)}{4 \cdot E_g \cdot 2 t_g} \tag{2}$$

where ε_c is the longitudinal strain of the CF/EP layer. The failure strain of the carbon fibres (quoted by the manufacturer) was used for ε_c as a rough estimation of the composite failure strain for design purposes. If G_{II} at first CF/EP layer fracture is lower than G_{IIC}, the continuous hybrid laminate can start accumulating damage by CF/EP layer fragmentation and stable delamination around the CF/EP fractures. Otherwise a major load-drop and delamination takes place at the first CF/EP fracture. In the case of the discontinuous hybrid laminates, delamination takes place when G_{II} exceeds G_{IIC}. In order to avoid catastrophic failure of the whole hybrid laminate at the moment the central carbon layer breaks, the outer glass layers are required to have a minimum layer thickness ($t_{g,min}$) [10]:

$$t_{g,min} = \frac{E_c \cdot \varepsilon_c \cdot t_c}{2 \cdot E_g \cdot (\varepsilon_g - \varepsilon_{2c})} \tag{3}$$

where ε_g = 3.41 [%] is the longitudinal tensile failure strain of the pristine SGF/EP layer based on our measurements (see section 3.3.). Please note that this value is conservative as the failure strain of the glass/epoxy was reduced by stress concentrations at the grips. The results of the design calculations are summarised in Table 3.

The critical energy release rate at room temperature is around $G_{IIC} = 1 \frac{N}{mm}$ based on experiments on similar material combinations and specimen thicknesses [37]. Please note, that the failure strain of the CF/EP layer in our continuous hybrid specimens was found to be remarkably higher than the failure strain value given by the manufacturer for

Table 2
Cured ply properties of the applied UD prepregs.

Prepreg material (Manufacturer)	Nominal fibre areal density[a] [g/m²]	Fibre volume fraction[a] [%]	Cured ply thickness[b] [μm]	Coefficient of thermal expansion[b] [1/°C]	Initial modulus[b] [GPa]
TC35 carbon/epoxy (SK Chemicals)	20	40	27.7	$8.57 \cdot 10^{-7}$	98.0
S-glass/epoxy (Hexcel)	190	49	153.8	$6.27 \cdot 10^{-6}$	45.6

[a] Based on manufacturer's data.
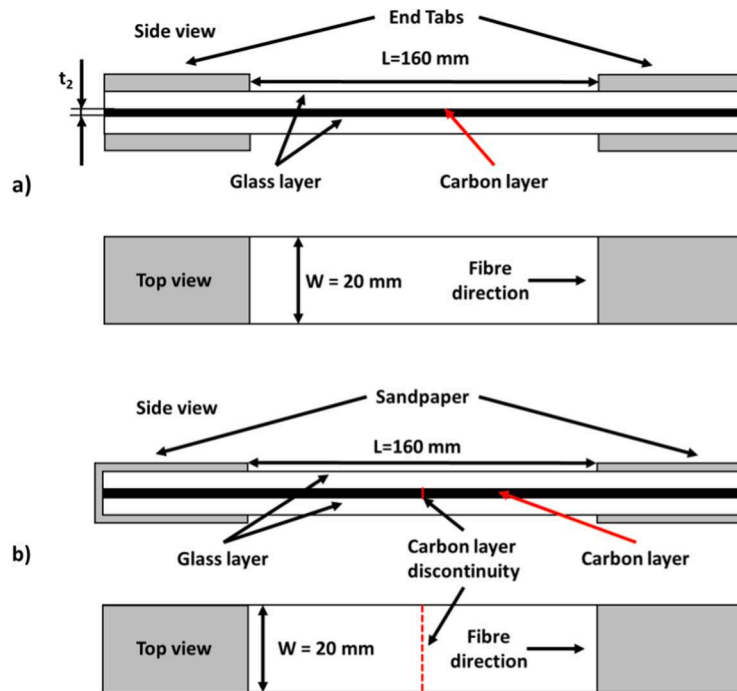[b] Calculated using manufacturer's data.

Fig. 1. Schematic of the a) continuous and b) discontinuous hybrid specimen geometry.

the fibres (i.e. around 2.1 % vs 1.6 %). The most probable reason for this observation is the hybrid effect present in thin-ply hybrid laminates [38] or simply the conservative approach of the fibre material provider. Hence, the values of G_{II} at CF/EP layer failure for both continuous and discontinuous hybrid specimens were predicted for two different strain values i.e. 1.6 % (CF failure strain according to the manufacturer) and 2.1 % (experimental failure strain of the CF/EP layer in our continuous hybrid laminates). All predicted G_{II} values (i.e. 0.480 and 0.959 N/mm at 1.6 % strain and 0.826 and 1.652 N/mm at 2.1 % strain) were included in Table 3 for completeness. Based on our design calculations, the continuous hybrid specimens should fragment and delaminate stably as G_{II} at CF/EP layer fracture is lower than G_{IIC} (i.e. 0.826 vs 1 N/mm). In case of the thicker, discontinuous specimens, the realistic G_{II} at CF/EP layer fracture is greater than the estimated G_{IIC}, (i.e. 1.652 N/mm vs 1 N/mm) therefore delamination is expected before CF/EP layer failure. To investigate the moisture sensitivity of the outer glass layers of the hybrids, monolithic unidirectional SGF/EP composite specimens ([S-glass₄]) were manufactured as well.

2.3. Manufacturing

The UD prepreg plies were put on top of each other according to the lay-up sequences (see Table 3). The vacuum bagged laminates were cured in an autoclave for 2 h at 125 °C and 0.7 MPa pressure. The temperature was monitored using thermocouples attached to the plates.

The matrix materials in the prepregs were both 125 °C cure epoxy resins. No details of the chemical formulation of the matrix materials were given by the prepreg manufacturers, but the resin systems in the hybrid laminates were found to be compatible. After curing, all the laminates were visually inspected and found suitable for specimen fabrication. 20 mm wide, parallel edge specimens were cut with a diamond cutting wheel.

2.4. Specimen conditioning and mechanical test procedure

After cutting the parallel edge specimens, half of the continuous and discontinuous hybrid specimens (15–15 respectively) were left unconditioned at ambient laboratory conditions while the other half (30 in total) were dried in a Memmert HCP153 type environmental chamber at 60 °C for 48 h. Then the mass of the pre-conditioned test pieces was measured and set as a reference. These hybrid specimens were conditioned for 1350 h whereas the monolithic SGF/EP specimens for 125/500/1000/1350 h. For all specimen types, the conditioning parameters were 60 °C and 90 % relative humidity. The specimens were removed regularly from the climate chamber to record their relative mass increase. 15 continuous, 15 discontinuous and the additional 40 SGF/EP specimens, altogether 70 conditioned test coupons were prepared for mechanical testing. Before measuring their mass gain, the surface of the specimens was carefully wiped dry with paper tissues. The further drying of the specimens during the mass measurement was found to be

Table 3
Calculated properties of the designed unidirectional hybrid specimen types.

[Lay-up sequence] (Designation)	Nominal thickness	Energy release rate at CF failure strain (1.6 %)[a]/experimental CF/EP layer failure strain (2.1 %)	Required minimum vs nominal SGF/EP layer thickness	Predicted elastic modulus[a]
	[mm]	[N/mm]	[mm]	[GPa]
[S-glass$_1$/TC35$_2$/S-glass$_1$] (Continuous hybrid)	0.358	0.480/0.826	0.053/0.155	54.7
[S-glass$_2$/TC35(cut)$_4$/S-glass$_2$] (Discontinuous hybrid)	0.716	0.959/1.652	0.105/0.310	54.7
[S-glass$_4$] (Monolithic S-glass)	0.620	–	–	45.6

[a] Calculated using manufacturer's data.

negligible. After the last mass measurement 50 mm long glass fabric/epoxy tabs were bonded to the ends of the continuous hybrid and monolithic glass/epoxy specimens using two-component epoxy adhesives. The Araldite 2011 two component epoxy adhesive was suitable for low and room temperature testing but it softened at 80 °C, therefore it was replaced with Araldite 2014 for the specimens prepared to be tested at elevated temperature. Both type specimens were put back in the environmental chamber to 60 °C and 90 % RH whilst the adhesive was curing, thereby the drying of the test coupons during the curing of the adhesive was avoided. In the case of the discontinuous hybrid specimens, where end-tabbing was not necessary due to the earlier damage initiation and lower maximum stresses, sandpaper was secured to the gripping areas of the specimens to avoid damage from the sharp grip faces as well as slippage. Uniaxial tensile testing of the unconditioned and conditioned hybrid composite specimens was carried out at three different test temperatures: −50 °C, room temperature (25 °C) and 80 °C. A minimum of 5 specimens were tested from each type at all temperatures, while the monolithic SGF/EP specimens were tested only at room temperature. A Zwick Z250 type universal test machine, equipped with an environmental chamber (see Fig. 2), regularly calibrated 250 kN load cell and 100 kN rated Instron 2716–003 type manual wedge action grips were used for tensile testing. Liquid nitrogen cooling and electric heating were used to set the desired test temperatures in the chamber. A crosshead speed of 4 mm/min was applied for the displacement controlled tensile tests. A Zwick BW40220 type video extensometer was used for strain measurement with a nominal gauge length of 75 mm.

2.5. Thermal effects in the tested hybrid laminates

In the case of the continuous hybrid specimens, the effect of thermal residual strains needs to be taken into account because the damage accumulation in the continuous specimen type governed by the multiple fracturing (fragmentation) of the carbon layer is affected by residual stress in the carbon. Due to the mismatch between the coefficients of thermal expansion (CTE) of the glass and carbon fibres, the CF/EP layers are loaded in compression in the cured hybrid composite, which results in apparent failure strain enhancement. The larger the difference between cure and test temperatures, the greater the apparent failure strain improvement. The damage initiation of the discontinuous specimens depends on the delamination onset, which takes place before carbon layer fragmentation (except for some specimens at −50 °C), and so is not directly affected by fragmentation. G_{IIC} is estimated from eq (2) substituting the damage initiation strain without correction for thermal strains since basic strain energy calculations showed that the contribution of residual stresses to G_{II} is negligible. In the case of the continuous specimens, the CTE of the monolithic composite layers (4) and the CTE of the hybrid composite (5) were calculated first, based on the rule of mixtures [39]:

$$\alpha_{comp} = v_f \cdot \alpha_f \cdot \frac{E_f}{E_{comp}} + \left(1 - v_f\right) \cdot \alpha_m \cdot \frac{E_m}{E_{comp}} \tag{4}$$

$$\alpha_h = \frac{t_c}{h} \cdot \alpha_c \cdot \frac{E_c}{E_h} + \left(1 - \frac{t_c}{h}\right) \cdot \alpha_g \cdot \frac{E_g}{E_h} \tag{5}$$

where α_{comp} is the coefficient of thermal expansion of the cured ply, α_f is the nominal CTE of the fibre, α_m is the CTE of the resin, v_f is the fibre volume fraction, E_f and.

$E_m = 3.4$ GPa(based on manufacturer's data sheet) are the nominal tensile moduli of the fibre and the matrix, E_{comp} is the nominal tensile modulus of the cured ply. In eq. (5) α_h is the calculated CTE of the hybrid, α_c and α_g are the calculated CTEs of the CF/EP and SGF/EP plies, $\frac{t_c}{h}$ is the volume fraction of the CF/EP in the hybrid laminate. Applying the above-mentioned formula, the CTE of the hybrid composites was $4.77 \bullet 10^{-6}$. In the next step the thermal strain of the hybrid material (6) was calculated. After that, the free thermal strain of the monolithic CF/EP layer was subtracted from the thermal strain of the hybrid in order to get the thermal residual strain of the carbon layer in the hybrid (7). Finally, the subtraction of the thermal residual strain from the measured damage initiation strain of the continuous hybrid gave the corrected failure strain of the CF/EP layer (8).

$$\varepsilon_{h,t} = \alpha_h \cdot \Delta T = \alpha_h \cdot \left(T_{cure} - T_{test}\right) \tag{6}$$

$$\varepsilon_{c,t} = \varepsilon_{h,t} - \varepsilon_{c,free} = \alpha_h \cdot \Delta T - \alpha_c \cdot \Delta T \tag{7}$$

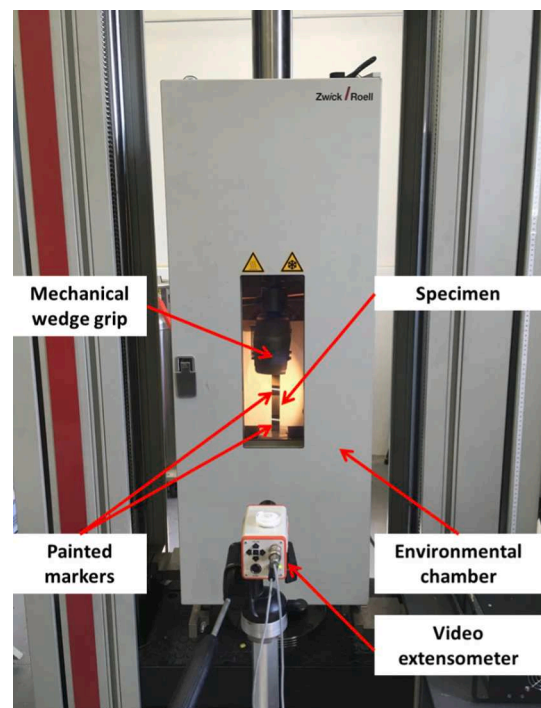**Fig. 2.** Test setup.

$$\varepsilon_{corr} = \varepsilon_d - \varepsilon_{c,t} \tag{8}$$

In eq. (6) $\varepsilon_{h,t}$ stands for the thermal strain of the hybrid, and ΔT is the temperature difference between cure and test temperatures. In eq. (7) $\varepsilon_{c,t}$ is the thermal residual strain of the CF/EP layer in the hybrid, $\varepsilon_{c,\ free}$ is the free thermal strain of the monolithic CF/EP. ε_{corr} stands for the corrected strain while ε_d is the measured damage initiation strain of the continuous hybrid.

3. Results and discussion

3.1. Water uptake processes of the different specimen types

The specimens were taken out of the environmental chamber at regular intervals to measure their mass to calculate the relative mass increase:

$$\Delta m = \frac{m - m_0}{m_0} \cdot 100 \ [\%] \tag{9}$$

where Δm is the relative mass increase, m is the measured actual mass of the specimen and m_0 is the measured initial mass. Based on the Lucas-Washburn equation, Vas and Nagy [40] developed a function (10) which was applied successfully earlier to model the water uptake process of fibre reinforced polymer composites:

$$\Delta m(t) = \Delta m_\infty \cdot \left(1 - e^{(-A \cdot t)^{\frac{1}{2K}}}\right)^K \rightarrow \Delta m_\infty, \ t \rightarrow \infty \tag{10}$$

In eq. (10) Δm_∞ is the relative mass increase of the specimen at infinite time (i.e. saturation), e is the base of the natural logarithm, t is the conditioning time in [h], A and K are material dependent constant parameters. This function, which provides an asymptotically correct approximation of the water uptake process in the case $t \rightarrow 0$ as well as $t \rightarrow \infty$, was fitted to the experimental data (Fig. 3), and was found to be suitable to model the water uptake process of both types of SGF/CF-EP hybrid, as well as the monolithic SGF/EP specimens. The data points in Fig. 3 represent the average of 15 continuous, 15 discontinuous hybrid and 8 monolithic SGF/EP specimens. The least squares fitting method was applied for curve fitting of the measured water uptake data points. For curve fitting purposes the data points were weighted according to the measurement time intervals to compensate for the variable data point density and achieve a better fit. It can be seen in the curves that the process is more rapid initially in the case of the thinner continuous specimens. Besides the capillary effect (i.e. water penetrates into the composite at the cut edges along the reinforcement fibres), a significant part of the absorbed water could have diffused into the specimens through the thickness, and in the case of the thinner specimens the surface/volume ratio is around double, which made the paths towards the centre shorter, explaining the more rapid water uptake. The similar relative mass increase values of the two hybrid specimen types suggest that their water uptake at saturation is similar, as expected based on their similar composition. Despite containing the same number of SGF/EP plies, the relative mass increase of the monolithic specimens was higher than that of the discontinuous hybrids.

The curve fitting parameters can be found in Table 4. The higher the value of parameter A, the steeper the initial section of the curve. In the case of the double thickness discontinuous specimens, the value of the parameter A is more than twice as high as that of the thinner continuous specimens. The fitted curve of the discontinuous specimens is also steeper in the initial stage. The lower the value of fitting parameter K the sharper the transition between the initial and the plateau stages of the water uptake curve. The discontinuous hybrid specimens and the monolithic SGF/EP specimens contained the same number of glass plies which might be the reason for similar K values of the fitted water uptake curves. Similar Δm_∞ values for the hybrid specimens indicate that the initial effect of the thickness gradually fades away. This is in line with our expectation, that the mass increase at saturation for materials with the same composition should be the same regardless of minor differences in geometry.

3.2. Effect of test temperature and moisture on the damage mode and the damage initiation strain of continuous thin-ply glass/carbon hybrid composites

As expected, the unconditioned continuous specimens showed non-linear pseudo-ductile behaviour in the whole temperature range (-50 °C to 80 °C). The central carbon layer fragmented and local delamination took place in the vicinity of the cracks (Fig. 4). The translucent

Table 4
Parameters of curve fitting to the water uptake experimental data of the conditioned specimens.

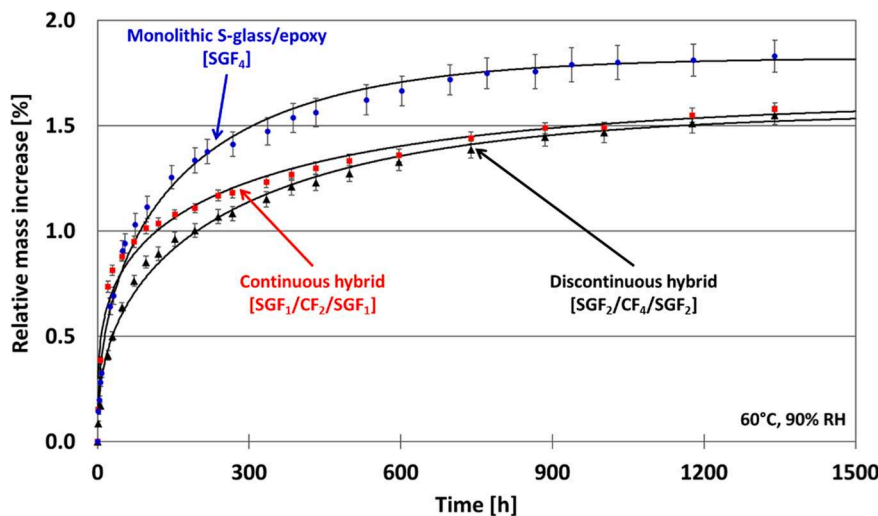| Specimen type	Curve fitting parameters (for eq. (10))		
	Δm_∞	A	K
Continuous hybrid	1.621	$0.717 \cdot 10^{-3}$	0.256
Discontinuous hybrid	1.565	$0.158 \cdot 10^{-2}$	0.397
Monolithic S-glass	1.822	$0.267 \cdot 10^{-2}$	0.416

Fig. 3. Water uptake results of the continuous hybrid, discontinuous hybrid and monolithic S-glass specimens with fitted curves.
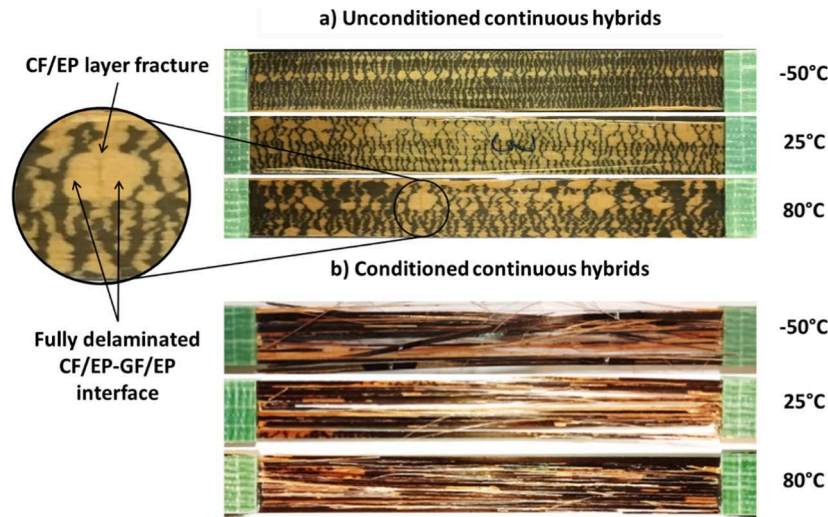
Fig. 4. Specimens with continuous carbon layer after the tensile tests: a) fragmentation of the carbon/epoxy layer and localised delamination between glass/epoxy and carbon/epoxy layers (Unconditioned), b) sudden, catastrophic failure (Conditioned).
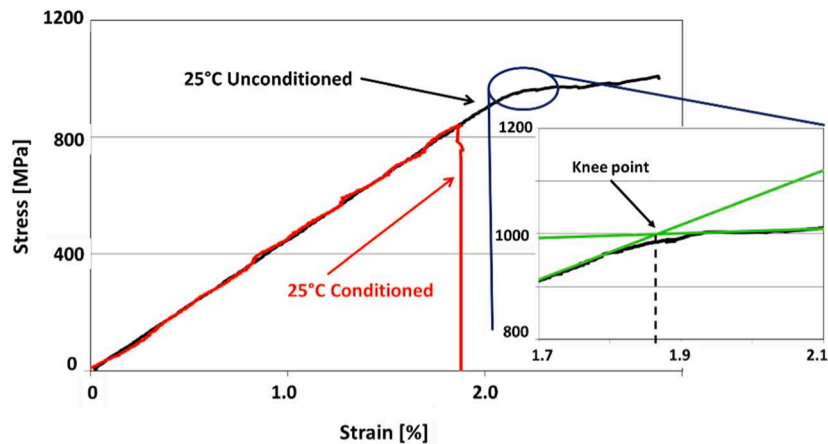

Fig. 5. The stress–strain response of typical unconditioned and conditioned continuous glass/carbon hybrid specimens and the definition of the knee point.
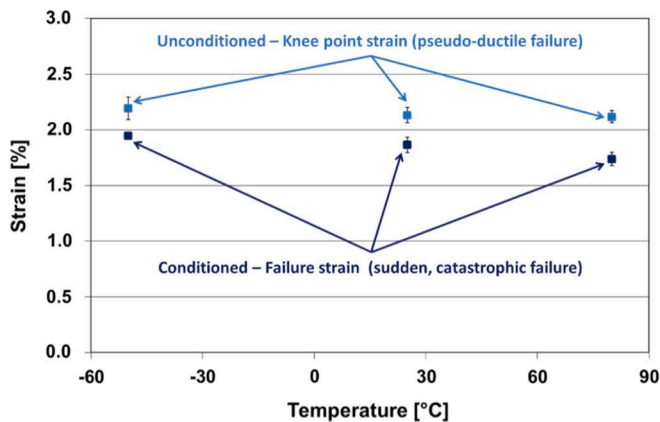

Fig. 6. Knee point strain/failure strain of continuous hybrid specimens as a function of test temperature and hot-wet conditioning.

nature of the GF/EP composite layer allowed for in-situ visual observation of the fragmentation process. The hybrid specimens originally had a dark colour because the black CF/EP layers were visible through the translucent GF/EP top layers. Delaminated areas changed their colour to yellow, because a new uneven surface was created between the GF/EP and CF/EP layers, letting the original colour of the GF/EP layer dominate. The dark areas of the specimens in Fig. 4a show the remaining bonded regions of the hybrid specimens.

The damage initiation was analysed by finding the knee point of the recorded stress–strain curves, which is defined by the intersection of straight lines fitted to the initial linear sections and the nearly horizontal plateaus (see definition in Fig. 5). The strains of the continuous specimen series in Fig. 6 were corrected with thermal residual strains as explained in section 2.5. The strain at the knee point (ε_{KP}) was barely affected by changing the temperature (see Fig. 6.). The main reason for this is that the tensile response of the continuous type specimens was dominated by the behaviour of the fibres which is insensitive to test temperature in the range of our study. After the central carbon layer has fully fragmented, the test was aborted to avoid final failure of the hybrid specimens, thereby allowing for visual observation of the fracture
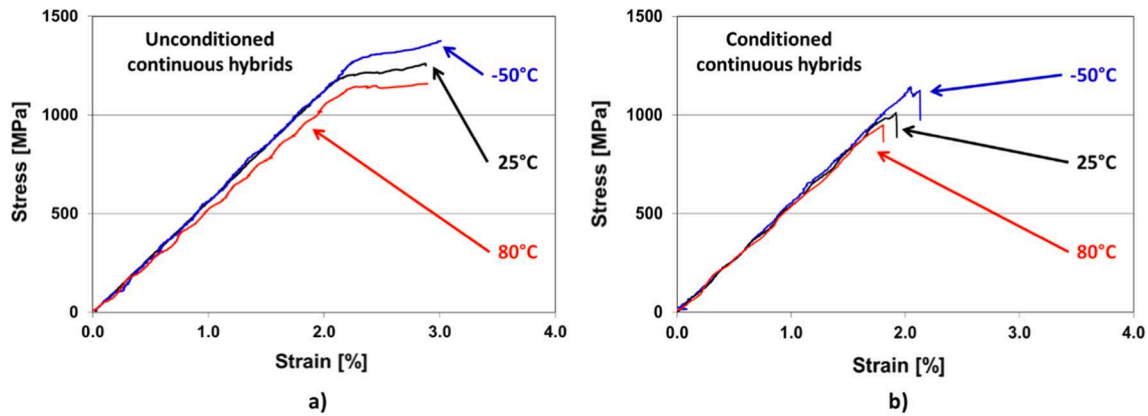
Fig. 7. Stress–strain curves of a) unconditioned continuous hybrid specimens and b) conditioned continuous hybrid specimens at all test temperatures.

Table 5
Tensile properties of conditioned and unconditioned continuous hybrid specimens at all temperatures.

Test temperature [°C] (Unconditioned)	Measured modulus from nominal thickness [GPa] (CoV [%])	Knee point stress from nominal thickness [MPa] (CoV [%])	Measured knee point strain [%] (CoV [rel. %])	Thermal strain corrected knee point strain [%] (CoV [rel. %])
−50	54.4 (4.9)	1256.4 (4.7)	2.26 (4.5)	2.19 (4.6)
25	54.6 (3.3)	1197.4 (2.8)	2.17 (3.1)	2.13 (3.2)
80	52.4 (2.0)	1146.0 (3.0)	2.14 (2.6)	2.12 (2.6)

Test temperature [°C] (Conditioned)	Measured modulus from nominal thickness [GPa] (CoV [%])	Tensile strength from nominal thickness [MPa] (CoV [%])	Measured failure strain [%] (CoV [rel. %])	Thermal strain corrected failure strain [%] (CoV [rel. %])
−50	56.0 (3.6)	1111.8 (3.1)	2.01 (1.6)	1.94 (1.7)
25	55.0 (4.0)	1048.2 (3.9)	1.90 (3.7)	1.86 (3.7)
80	54.7 (3.2)	957.9 (1.2)	1.75 (3.5)	1.74 (3.5)

patterns (see Fig. 4a).

Please note, that the knee point indicates the onset of the progressive failure and not the first carbon layer fracture which is also believed to be unaffected by temperature change between −50 °C and 80 °C. At low temperature, small delaminated areas were localized in the vicinity of the first few CF/EP layer cracks and did not change the stiffness of the hybrid specimens until higher applied strains. On the other hand, at high temperature, larger delaminated zones appeared (see Fig. 4a), which were more capable of reducing the specimen stiffness immediately and therefore brought the knee point strain slightly lower (see Fig. 7).

Hot-wet conditioning hindered the pseudo-ductile behaviour and sudden, catastrophic failure took place (Fig. 5). Since the first macroscopic carbon layer fracture caused overall failure of the conditioned specimens, more than 10 % strain reduction was observed at all temperatures compared to the knee point strain values of the unconditioned continuous hybrids (Fig. 6). It is hypothesised based on post mortem observation of the specimens and videos recorded during the tests, that

two competing damage mechanisms were active at the same time leading to abrupt failure of the conditioned continuous hybrid specimens: i) The glass/epoxy layers were overloaded and broke at the first few local carbon layer fractures resulting in splitting of the whole specimen (see Fig. 4b). ii) The glass/epoxy layers were also overloaded near the end-tabs by the stress concentrations from the grips and could fracture and split from there before the carbon layer started fragmenting (see Fig. 4b).

Brush-like splitting starting from the edge of the tabs was dominant in the case of the conditioned specimens at −50 °C. At room temperature, the brush type failed specimens indicated that the failure of the SGF/EP bundles initiated either from the edges of the tabs or from CF/EP layer fractures within the gauge section. Traces of fragmentation were also detected (see Fig. 4). Fragmentation was more pronounced at 80 °C while splitting originated from the tab region or from CF/EP fractures in the gauge section still played a significant role in the damage process. The obvious change in the failure mode suggests a significant reduction

Table 6
The effect of hot-wet conditioning on the tensile mechanical properties of monolithic glass/epoxy composites at room temperature.

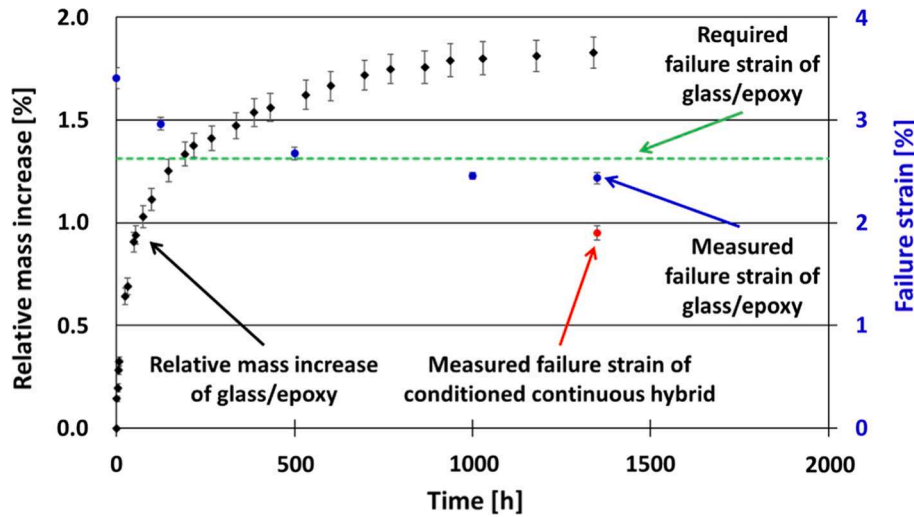| Conditioning at 60 °C, 90 % RH	Measured modulus from nominal thickness [GPa] (CoV [%])	Failure strain [%] (CoV [rel.%])	Tensile strength from nominal thickness [MPa] (CoV [%])
pristine	46.7 (2.5)	3.41 (3.1)	1551.8 (4.5)
125 h	46.1 (4.4)	2.96 (2.1)	1344.5 (6.0)
500 h	46.2 (3.3)	2.68 (2.3)	1237.2 (3.5)
1000 h	46.3 (3.8)	2.46 (1.3)	1133.6 (3.3)
1350 h	46.9 (3.5)	2.44 (2.4)	1133.2 (4.4)

Fig. 8. Moisture induced degradation and the resulting decrease of the failure strain of UD monolithic SGF/EP specimens.

in the strength of the S-glass/epoxy layers due to wet conditioning. Therefore, the residual strength of the SGF/EP composite after long term exposure to moisture was investigated further and is discussed in detail in the following section. The tensile properties of both types of continuous hybrids at all temperatures are summarized in Table 5.

3.3. Effect of hot-wet conditioning on the strength of S-glass/epoxy

GF/EP composites are reported to be sensitive to moisture absorption [25–28]. Wet conditioning causes matrix plasticisation which leads to reduction in mechanical properties such as stiffness and tensile strength. In the case of neat epoxy, the effects of plasticisation are reversible through drying [41]. Long term exposure to moisture may cause permanent degradation of the fibre–matrix interface [42,43], that could lead to insufficient stress transfer between the fibres and the matrix. In addition, the presence of moisture can reduce the strength of glass fibres through leaching of soluble elements [44]. Stress corrosion of glass fibres may occur when they are exposed to moisture and tensile stresses at the same time. Stress corrosion cracking may have affected our wet conditioned hybrid laminates since the GF/EP layers are loaded in tension in the hybrid material due to thermal residual stresses.

In order to investigate the reason for the observed change of failure mode in the conditioned continuous hybrid laminates from fragmentation to catastrophic overall fracture, we ran a separate study. Monolithic SGF/EP UD composite specimens were prepared and conditioned for 125/500/1000/1350 h at 60 °C and 90 % RH to investigate the effect of hot-wet conditioning on their longitudinal tensile properties and explore the reason for the abrupt failure of the conditioned continuous hybrid specimens. Whilst the tensile modulus of the SGF/EP composite did not change, both their tensile strength and failure strain decreased with

Fig. 9. Tensile stress concentration in the glass/epoxy layers in the vicinity of carbon layer fracture (delamination is neglected).

conditioning time by up to 28 % after 1000 h (see Table 6 andFig. 8).

UD composites show quasi-linear tensile stress–strain response, therefore a very simple mechanical model based on Hooke's law (11) was applied to specify the required failure strain of the SGF/EP layers at the failure strain of the embedded CF/EP layer in the continuous hybrid specimens. For simplification the model neglects the local delamination in the vicinity of the first crack in the carbon layer and assumes constant strain through the thickness of the hybrid laminates prior to carbon layer fracture.

$$\sigma_{eff} = \frac{F}{A_h} = E_h \cdot \varepsilon \rightarrow F = E_h \cdot \varepsilon \cdot A_h \tag{11}$$

In eq. (11) σ_{eff} is the effective tensile stress calculated based on F, the full tensile force on the specimen and A_h the hybrid specimen's full cross-section, E_h is the tensile elastic modulus of the hybrid specimen, ε is the strain of the hybrid specimen which is assumed to be constant through the thickness until the first fracture in the CF/EP layer. A force equilibrium (12) can be written at the moment of the first carbon layer fracture (Fig. 9): before the first CF/EP layer fracture the whole cross-section of the specimen carries the load (left side of eq. (12)), while after the first fracture only the SGF/EP layers take the load in the vicinity of the crack (right side of eq. (12)).

$$E_h \cdot \varepsilon_{bc} \cdot A_h = E_g \cdot \varepsilon_{g(bc)} \cdot A_g \tag{12}$$

In eq. (12) A_h and A_g are the full cross-sectional area of the continuous hybrid and the glass layers respectively, ε_{bc} is the breaking strain of carbon layer in the hybrid, $\varepsilon_{g(bc)}$ is the strain of the glass layers at the breaking strain of the carbon layer (after breakage), E_1 is the elastic modulus of the cured glass/epoxy plies. Rearranging eq. (12) to the ratio of first carbon fracture strain and minimum glass failure strain, substituting eq. (1) to E_h and using the known geometric parameters, the magnitude of the strain increment in the S-glass/epoxy layers can be calculated:

$$\frac{\varepsilon_{g(bc)}}{\varepsilon_{bc}} = \frac{E_h \cdot A_h}{E_g \cdot A_g} = \frac{\frac{E_g \cdot 2 \cdot t_g + E_c \cdot t_c}{h}(h \cdot w)}{E_g \cdot 2 \cdot t_g \cdot w} = \frac{E_g \cdot 2 \cdot t_g + E_c \cdot t_c}{E_g \cdot 2 \cdot t_g} = 1.38 \tag{13}$$

where E_h is the initial elastic modulus of the hybrid, E_g and E_c are the elastic moduli of the SGF/EP and CF/EP layers in the fibre direction, h is the overall thickness of the specimen, t_g and t_c are the thickness of the SGF/EP and the CF/EP layers and w is the width of the hybrid specimen. Multiplying the measured failure strain of the conditioned continuous hybrid specimen at room temperature (1.90 %) with the strain ratio
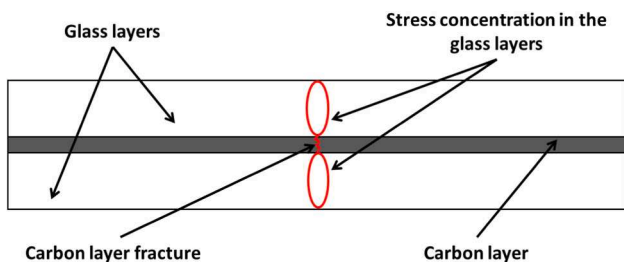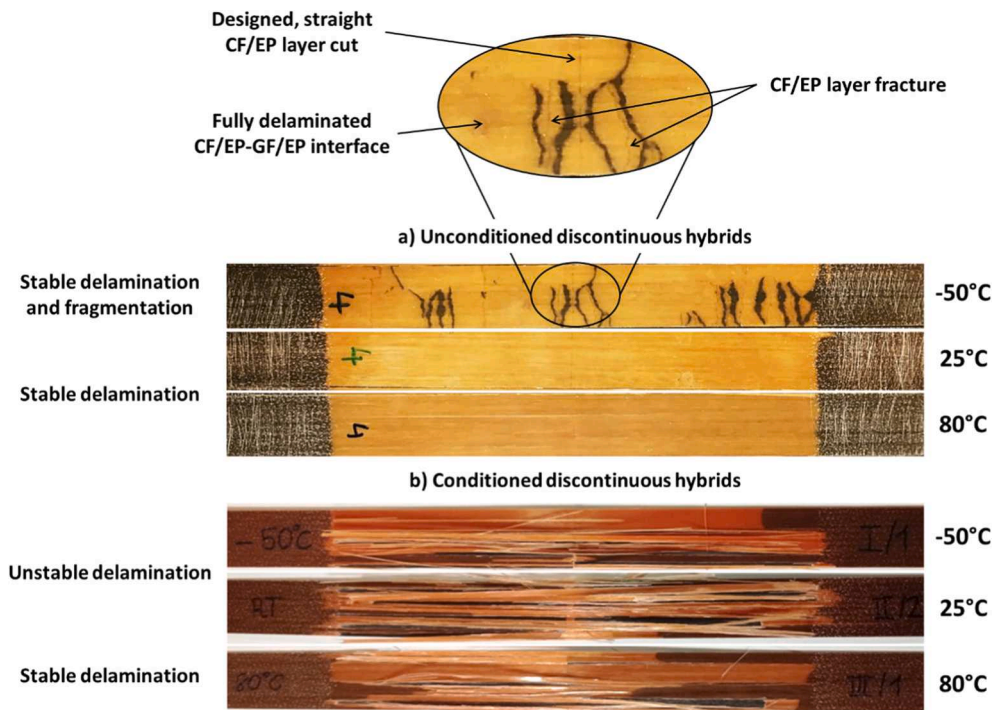
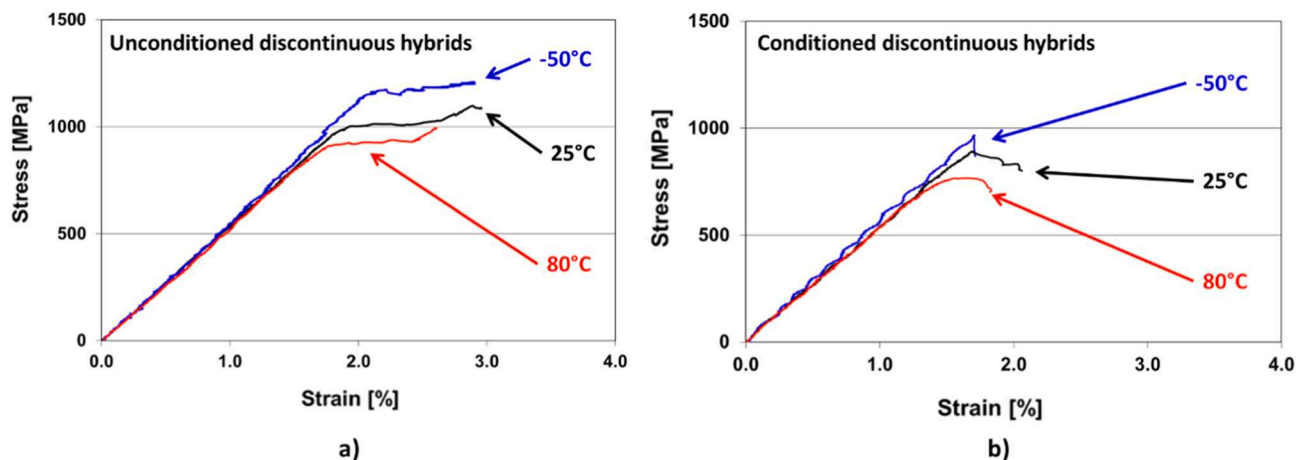**Fig. 10.** Failed hybrid specimens with discontinuous CF/EP layer.

Fig. 11. Stress–strain curves of the (a) unconditioned discontinuous hybrid and (b) conditioned discontinuous hybrid specimens at various temperatures.

from eq. (13), the minimum required failure strain of the glass/epoxy layers is 2.63 % to avoid catastrophic failure of the continuous hybrid. The reason for the lack of pseudo-ductility in the case of the conditioned continuous hybrid specimens after 1000 h is that the failure strain of the conditioned monolithic SGF/EP composite is lower (2.46 %) than the minimum required breaking strain according to Fig. 8. which still ignores stress concentrations due to the broken carbon and stress transfer from the grips. Thus the glass layers were unable to bear the additional load after the first few carbon layer fracture and started to break locally and split, triggering the catastrophic overall failure of the specimens. A second, competing failure mechanisms may have been the fracture and splitting of the glass layers near the end tabs where significant stress concentrations were also present, this case due to shear load transfer from the grips. Visual investigation and videos recorded during the tests indicated that most probably both mechanisms were active during the failure process.

3.4. Effect of test temperature and moisture on the interlaminar fracture toughness of the hybrid laminates

The unconditioned discontinuous hybrid specimens delaminated stably at room and high temperature as expected (see Fig. 10). As a result of delamination propagation from the central cut, the optical properties of the specimen changed and the initially bonded, dark gauge section turned yellow gradually. Hence, the translucent nature of the GF/EP composite layer allowed for in-situ visual observation of the delamination propagation between the GF/EP and CF/EP layers. The yellow areas of the unloaded unconditioned discontinuous specimens after the test were fully delaminated (see Fig. 10). We confirmed this by separating their three layers, which was easy to do by hand. The stable delamination propagation is indicated by the gradual stiffness change (i. e. flat plateau) in the stress–strain graphs (Fig. 11/a). However, delamination and carbon layer fragmentation occurred at the same time at −50 °C due to the increased mode II interfacial properties. 3 out of 5
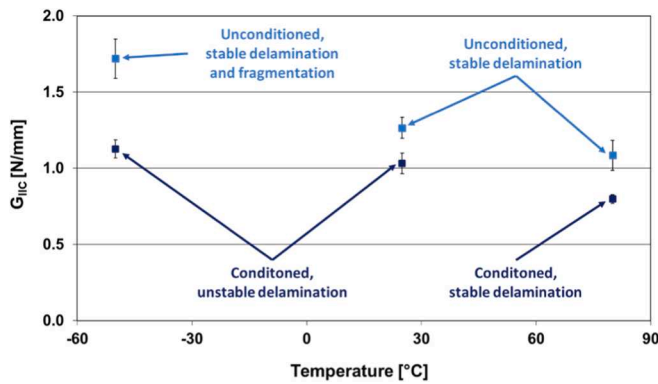
Fig. 12. The effect of test temperature and moisture on the mode II fracture toughness.

of the tested specimens delaminated fully, while the rest of them showed traces of fragmentation beside delamination. No significant effect of the observed fragmentation on the knee-point strain was found during the analysis of the test data. In turn, at low temperature, wet conditioning changed the damage mode: the glass and carbon layers delaminated unstably in the conditioned discontinuous specimens leading to significant load drops in the stress–strain curves (see Fig. 11/b). In some cases, unstable delamination was followed by the splitting of SGF/EP layers. On one hand, some of the glass fibre bundles failed in the vicinity of the CF/EP layer discontinuity because in that region only the SGF/EP layers carried the load. On the other hand, some fractures of the SGF/EP layers appeared near the grips due to stress concentration. The early appearance of the SGF/EP layer fractures confirms that the absorbed moisture reduced their strength.

The mode II fracture toughness G_{IIC} was calculated by a modified form of eq. (2), where ε_{KP} stands for the measured knee point strain of the discontinuous specimens, at which delamination initiated:

$$G_{IIC} = \frac{\varepsilon_{KP}^2 \cdot E_c \cdot t_c (E_g \cdot 2 \cdot t_g + E_c \cdot t_c)}{4 \cdot E_g \cdot 2 t_g} \tag{14}$$

The test results clearly show that the knee point strain and the mode II fracture toughness of the unconditioned discontinuous hybrid specimens decreases at high temperature and increases at low temperature (Figs. 11 and 12), with stable delamination generally initiating from the designed central cut.

Wet conditioned specimens tested at −50 °C showed unstable delamination and splitting in parallel. Premature glass fibre failure (investigated in section 3.3.) and the induced extensive splitting of the specimens may have yielded a lower bound estimation of G_{IIC}. The conditioned specimens tested at room temperature, first started to delaminate and then the glass layers failed by splitting at highly loaded regions of the specimens (i.e. at the discontinuity in the CF/EP layer and near the grips, see Fig. 11/b). In case of the conditioned discontinuous specimens tested at 80 °C, delamination initiated stably, while the measured knee point and final failure strain was lower than those of the unconditioned specimen types. Scattered splitting of the SGF/EP layers restricted the complete delamination of the glass-carbon interface. Similarly to [30] and [32], water absorption of the epoxy matrix composite specimens decreased the mode II fracture toughness. The effect of higher test temperature on the estimated values of G_{IIC} is also in line with the reported decreasing trends found in the literature [31,33].

4. Conclusions

In the present paper the combined effect of test temperature (-50, 25, 80 °C) and moisture (long term 90 % RH at 60 °C) on the pseudo-ductility of unidirectional thin-ply glass/carbon-epoxy hybrid composites was investigated. The following conclusions were drawn:

- Unconditioned hybrid specimens showed pseudo-ductile stress–strain response between −50 °C and 80 °C: the continuous specimens fragmented, and the discontinuous specimens delaminated stably between the glass and carbon layers.
- The mode II fracture toughness, which has been estimated from the delamination stress of specimens with a cut, was significantly decreased with increasing test temperature.
- Water uptake of monolithic SGF/EP and both continuous and discontinuous hybrid specimens was investigated in detail during long term exposure to 60 °C and 90 % relative humidity and a suitable function was found which fitted the experimental data well.
- Wet conditioning at 60 °C eliminated the pseudo-ductile behaviour of the continuous hybrid composites, and sudden failure occurred instead of progressive damage accumulation before final failure at all test temperatures. The reason for the absence of pseudo-ductility was found from the results of monolithic SGF/EP tensile tests: The strength of the glass composite was significantly reduced due to long-term hot-wet conditioning.
- The absorbed moisture decreased the estimated mode II fracture toughness, which is consistent with other reported results.
- Improved moisture resistance of glass/epoxy composites or a greater margin in the design of the layup is required to sustain the pseudo-ductile behaviour of these thin-ply hybrid laminates under wet conditions. All-carbon thin-ply hybrid composites may be more suitable to withstand environmental effects.

CRediT authorship contribution statement

Gergely Czél: Conceptualization, Methodology, Writing – review & editing, Supervision, Funding acquisition. **Márton Bugár-Mészáros:** Methodology, Investigation, Writing – original draft, Visualization. **Michael R. Wisnom:** Conceptualization, Writing – review & editing, Funding acquisition.

Declaration of Competing Interest

The authors declare that they have no known competing financial interests or personal relationships that could have appeared to influence the work reported in this paper.

Data availability

Data will be made available on request.

Acknowledgement

References

[1] Boncel S, Sundaram RM, Windle AH, Koziol KKK. Enhancement of the mechanical properties of directly spun CNT fibres by chemical treatment. ACS Nano 2011;5: 9339–44.

[2] Kumar R, Rai B, Gahlyan S, Kumar G. A comprehensive review on production, surface modification and characterization of nanocellulose derived from biomass and its commercial applications. Express Polym Lett 2021;15:104–20.

[3] Callens MG, Gorbatikh L, Verpoest I. Ductile steel fibre composites with brittle and ductile matrices. Compos Part A 2014;61:235–44.

[4] Callens MG, Gorbatikh L, Bertels E, Goderis B, Smet M, Verpoest I. Tensile behaviour of stainless steel fibre/epoxy composites with modified adhesion. Compos Part A 2015;69:208–18.

[5] Fuller JD, Wisnom MR. Pseudo-ductility and damage suppression in thin ply CFRP angle-ply laminates. Compos Part A 2015;69:64–71.

[6] Fuller JD, Wisnom MR. Exploration of the potential for pseudo-ductility in thin ply CFRP angle-ply laminates via an analytical method. Compos Sci Technol 2015;112: 8–15.

[7] Rév T, Jalalvand M, Fuller J, Wisnom MR, Czél G. A simple and robust approach for visual overload indication - UD thin-ply hybrid composite sensors. Compos A Appl Sci Manuf 2019;121:376–85.

[8] Czél G, Wisnom MR. Demonstration of pseudo-ductility in high performance glass-epoxy composites by hybridisation with thin-ply carbon prepreg. Compos A Appl Sci Manuf 2013;52:23–30.

[9] Czél G, Jalalvand M, Wisnom MR. Design and characterisation of advanced pseudo-ductile unidirectional thin-ply carbon/epoxy-glass/epoxy hybrid composites. Compos Struct 2016;143:362–70.

[10] Czél G, Jalalvand M, Wisnom MR, Czigány T. Design and characterisation of high performance, pseudo-ductile all-carbon/epoxy unidirectional hybrid composites. Compos B Eng 2017;111:348–56.

[11] Czél G, Rev T, Jalalvand M, Fotouhi M, Longana ML, Nixon-Pearson OJ, et al. Pseudo-ductility and reduced notch sensitivity in multi-directional all-carbon/ epoxy thin-ply hybrid composites. Compos A Appl Sci Manuf 2018;104:151–64.

[12] Marlett K. Hexcel 8552 IM7 unidirectional prepreg 190 gsm & 35% RC Qualification material property report. Wichita: National institute for aviation reshearch; 2011.

[13] Wu P, Xu L, Luo J, Zhang X, Bian W. Tension-tension fatigue performances of a pultruded carbon fiber reinforced epoxy plate at elevated temperatures. Compos Struct 2019;215:421–31.

[14] Miyano Y, Nakada M, Cai H. Formulation of long-term creep and fatigue strengths of polymer composites based on accelerated testing methodology. J Compos Mater 2008;42:1897–919.

[15] Nakada M, Miyano Y. Advanced accelerated testing methodology for long-term life prediction of CFRP laminates. J Compos Mater 2015;49:163–75.

[16] Nakada M, Miyano Y. Temperature dependence of statistical fatigue strengths for unidirectional carbon fiber reinforced plastics under tension loading. J Compos Mater 2020;54:1797–806.

[17] Koma A, Nakada M, Miyano Y. Temperature dependence of statistical static strengths for unidirectional CFRP with various carbon fibers. 18th European Conference on Composite Materials 2018.

[18] Haque A, Mahmood S, Walker L, Jeelani S. Moisture and temperature induced degradation in tensile properties of Kevlar-graphite/epoxy hybrid composites. J Reinf Plast Compos 1991;10:132–45.

[19] Ryan JM, Adams R, Brown SGR. Moisture ingress effect on properties of CFRP. 17th International Conference on Composite Materials. 2009.

[20] Selzer R, Friedrich K. Mechanical properties and failure behaviour of carbon fibre-reinforced polymer composites under the influence of moisture. Compos Part A 1997;28A:595–604.

[21] Nandagopal RA, Chai GB, Narasimalu S. An empirical model to predict the strength degradation of the hygrothermal aged CFRP material. Compos Struct 2020;236.

[22] Tual N, Carrere N, Davies P, Bonnemains T, Lolive E. Characterization of sea water ageing effects on mechanical properties of carbon/epoxy composites for tidal turbine blades. Compos Part A 2015;78:380–9.

[23] da Silva LV, da Silva FW, Tarpani JS, de Camargo Forte MM, Amico SC. Ageing effect on the tensile behavior of pultruded CFRP rods. Mater Des 2016;110:245–54.

[24] Robert M, Benmokrane B. Behavior of GFRP reinforcing bars subjected to extreme temperatures. J Compos Constr 2010;353–360.

[25] Ishai O. Environmental effects on deformation, strength and degradation of unidirectional glass-fiber reinforced plastics. II. Experimental Study. Polym Eng Sci 1975;15(7):491–9.

[26] Assarar M, Scida D, El Mahi A, Poilâne C, Ayad R. Influence of water ageing on mechanical properties and damage events of two reinforced composite materials: Flax–fibres and glass–fibres. Mater Des 2011;32:788–95.

[27] Wei B, Cao H, Song S. Degradation of basalt fibre and glass fibre/epoxy resin composites in seawater. Corros Sci 2011;53:426–31.

[28] Gibhardt D, Doblies A, Meyer L, Fiedler B. Effects of Hygrothermal Ageing on the Interphase, Fatigue, and Mechanical Properties of Glass Fibre Reinforced epoxy. Fibers 2019;7:55.

[29] Selzer R, Friedrich K. Influence of water up-take on interlaminar fracture properties of carbon fibre-reinforced polymer composites. J Mater Sci 1995;30: 334–8.

[30] Zhao S, Gaedke M. Moisture effects on mode II delamination behaviour of carbon/ epoxy composites. Adv Compos Mater 1996;5(4):291–307.

[31] Asp LE. The effects of moisture and temperature on the interlaminar delamination toughness of a carbon/epoxy composite. Compos Sci Technol 1998;58:967–77.

[32] Todo M, Nakamura T, Takahashi K. Effects of moisture absorption on the dynamic interlaminar fracture toughness of carbon/epoxy composites. J Compos Mater 2000;34:630–48.

[33] Sjögren LEA. Effects of temperature on delamination growth in a carbon/epoxy composite under fatigue loading. Int J Fatigue 2002;24:179–84.

[34] Landry G, LaPlante LRL. Environmental effects on mode II fatigue delamination growth in an aerospace grade carbon/epoxy composite. Compos Part A 2012;43: 475–85.

[35] Sengodan GA, Allegri G, Hallett SR. Simulation of progressive failure in laminated composites under variable environmental conditions. Mater Des 2020;196.

[36] Cui W, Wisnom MR, Jones M. An Experimental and Analytical Study of Delamination of Unidirectional Specimens with Cut Central Plies. J Reinf Plast Compos 1994;13:722–39.

[37] Czél G, Jalalvand M, Wisnom MR. Demonstration of pseudo-ductility in unidirectional hybrid composites made of discontinuous carbon/epoxy and continuous glass/epoxy plies. Compos Part A 2015;72:75–84.

[38] Wisnom MR, Czél G, Swolfs Y, Jalalvand M, Gorbatikh L, Verpoest I. Hybrid effects in thin ply carbon/glass unidirectional laminates: Accurate experimental determination and prediction. Compos Part A 2016;88:131–9.

[39] Czél G, Jalalvand M, Wisnom MR. Hybrid specimens eliminating stress concentrations in tensile and compressive testing of unidirectional composites. Compos Part A 2016;91:436–47.

[40] Czél G, Czigány T. A Study of Water Absorption and Mechanical Properties of Glass Fiber/Polyester Composite Pipes — Effects of Specimen Geometry and Preparation. J Compos Mater 2008;42:2815–27.

[41] Krauklis AE, Gagani AI, Echtermeyer AT. Hygrothermal Aging of Amine Epoxy: Reversible Static and Fatigue Properties. Open Engineering 2018;8:447–54.

[42] Rocha I, van der Meer FP, Raijmaekers S, Lahuerta F, Nijssen R, Mikkelsen LP, et al. A combined experimental/numerical investigation on hygrothermal aging of fiber-reinforced composites. Eur J Mech A Solids 2019;73:407–19.

[43] Rao V, Drzal LT. The dependence of interfacial shear strength on matrix and interphase properties. Polym Compos 1991;12:48–56.

[44] Krauklis A, Gagani A, Vegere K, Kalnina I, Klavins M, Echtermeyer A. Dissolution Kinetics of R-Glass Fibres: Influence of Water Acidity, Temperature, and Stress Corrosion. Fibers 2019;7:22.